

# High-resolution assessment of global technical and economic hydropower potential

David E. H. J. Gernaat<sup>1,2\*</sup>, Patrick W. Bogaart<sup>2</sup>, Detlef P. van Vuuren<sup>1,2</sup>, Hester Biemans<sup>1,3</sup> and Robin Niessink<sup>1,2</sup>

**Hydropower is the most important renewable energy source to date, providing over 72% of all renewable electricity globally. Yet, only limited information is available on the global potential supply of hydropower and the associated costs. Here we provide a high-resolution assessment of the technical and economic potential of hydropower at a near-global scale. Using 15"×15" discharge and 3"×3" digital elevation maps, we built virtual hydropower installations at >3.8 million sites across the globe and calculated their potential using cost optimization methods. This way we identified over 60,000 suitable sites, which together represent a remaining global potential of 9.49 PWh yr<sup>-1</sup> below US\$0.50 kWh<sup>-1</sup>. The largest remaining potential is found in Asia Pacific (39%), South America (25%) and Africa (24%), of which a large part can be produced at low cost (<US\$0.10 kWh<sup>-1</sup>). In an ecological scenario, this potential is reduced to 5.67 PWh yr<sup>-1</sup>.**

Hydropower currently supplies 16% of the world's total electricity and over 72% of all renewable electricity<sup>1</sup>. Its reliable energy production makes hydropower an attractive alternative to fossil-fuel-based technologies. Furthermore, thanks to the flexibility and energy storage capacity, some forms of hydropower can play a key role in balancing intermittent supply from solar and wind sources. However, despite these advantages, information on the potential future supply of hydropower is far less developed than for other renewable energy sources. While the literature includes several global assessments of solar and wind potential<sup>2–5</sup>, similar information on hydropower is still lacking. As a result, nearly all energy-economy models and publications on energy and climate change<sup>1, 6–8</sup> are confined to using the global estimates from the Hydropower Atlas<sup>9</sup>, which are based on a disparate range of national government surveys rather than a consistent global methodology.

Some earlier studies by the hydrological community have assessed theoretical global hydropower potential using runoff-weighted elevation differences based on low-resolution (0.5° × 0.5°) hydrological discharge data<sup>10–15</sup>. However, these estimates are far from realistic as they do not take into account local conditions or economic considerations. A recent study by Zhou et al.<sup>14</sup> aimed to improve these estimates by using a consistent, transparent method combining hydrological and economic data from the US hydropower industry. However, their assessment is based on low-resolution (0.5° × 0.5°) data, which means that all kinds of loss, in particular those related to resistance, are ignored. Local conditions, such as slope, geographical features and nearby land use, play a key role in the performance of hydropower systems. Hence, estimates based on runoff-weighted elevation differences at 0.5° × 0.5° resolution, such as reported by Zhou et al. (2015), are of limited practical value, also because the ratio between theoretical potential and maximum exploitable potential is largely unknown at this resolution. A more advanced, higher-resolution approach was used by Oak Ridge National Laboratory (ORNL)<sup>16</sup> assessing the hydropower potential along river segments in the United States based on a cascade-like system of small reservoirs. However, this method has not yet

been applied in a global assessment. Hence, current information on global hydropower potential is limited, either for methodological reasons (use of low-resolution data, focus on theoretical potential) or because it is available only for a specific region of the world.

Here, we provide a consistent, site-specific assessment of hydropower potential at a near-global scale (56° S to 60° N) using high-resolution discharge (15"×15") and elevation (3"×3") data. On the basis of this data, we evaluate hydropower installations at >3.8 million sites across the globe and calculate their technical and economic potential using cost optimization methods. This way we identify over 60,000 suitable sites, and estimate global hydropower potential based on the cumulative potential of these individual locations. By using high-resolution discharge and elevation data, our assessment directly takes into account a whole set of local conditions, including local topography, monthly discharge and land use. Moreover, by using cost planning tools developed by the hydropower industry, we are able to generate global and regional cost-supply curves, which is a significant step forward from existing studies that provide separate estimates for (often poorly defined) economic and technical potential.

## Assessing technical and economic hydropower potential

We used the high-resolution hydrographic maps of HydroSHEDS<sup>17</sup> (15"×15"; 450 m at the Equator) to downscale the available low-resolution (0.5° × 0.5°) runoff data (30 yr average 1970–2000) from the LPJmL hydrology and vegetation model<sup>18–21</sup>. Water demand from the agriculture, residential, industry and electricity sectors was subtracted in the downscaling routine<sup>22, 23</sup>. The resulting 15"×15" annual and monthly discharge maps were used to evaluate site-specific hydropower potential at every 25 km interval of every river between 56° S and 60° N (the excluded area is due to unavailable HydroSHEDS topographic data). At each site, we used high-resolution HydroSHEDS topographic data (3"×3"; 90 m at the Equator) to calculate the cost-optimal dimensions and associated production potential of two hydropower systems: river power plants and diversion canal power plants (following the definitions of Wagner and Mathur<sup>24</sup>). These systems have specific characteristics that are

<sup>1</sup>PBL - Netherlands Environmental Assessment Agency, Bezuidenhoutseweg 30, 2594 AV Den Haag, The Netherlands. <sup>2</sup>Copernicus Institute of Sustainable Development, Utrecht University, Heidelberglaan 2, 3584 CS Utrecht, The Netherlands. <sup>3</sup>Wageningen Environmental Research (Alterra), PO Box 47, 6700 AA Wageningen, The Netherlands. \*e-mail: david.gernaat@pbl.nl

suitable for different local conditions. River power plants harness energy mainly from the flow of the river and the head created by a dam. They have medium storage potential and some water reserves to serve medium to peak electricity load. Diversion canal power plants, which are often found in mountainous areas, are characterized by a water inlet at higher elevation diverting river water through pipes to a power station at lower elevation. These systems have no dam and therefore no storage capacity.

To assess the cost effectiveness of both these systems at each site, we used the 15°×15° discharge data and 3°×3° topographic data to feed cost equations derived from Norwegian and US hydropower tenders and contracts<sup>25,26</sup> (see Methods). The hydropower industry uses these equations as planning tools to calculate foreseeable contractor and supplier costs of projects in early planning stages. Our assessment considered the cost components for dam construction, turbines, pipes, powerhouses, fish mitigation, power lines, seismic risk, displacement costs and loss of agricultural land. To calculate the last two, we used LandScan population data (Bright et al., 2011) and current land use data from the IMAGE 3.0 model<sup>27</sup>, respectively. The latter is calibrated to FAO statistics on actual crop yields and crop areas<sup>28</sup>. To obtain the average generation costs (\$ kWh<sup>-1</sup>) for each system at each site, we divided the sum of all cost components by the energy production, which we calculated on the basis of local discharge, head and a load factor (annual hours of maximum turbine output). At each site, we optimized the dimensions of the dam (river power systems) and pipes (diversion canal power systems) using optimization methods to determine the trade-off between energy production and costs. For example, river power production was constrained by the cost categories discussed above through restricting dam height. This way, large reservoirs in urban areas were avoided because of high displacement costs. Finally, to avoid overlap between reservoirs, we used an optimization method to prioritize dam sites with the lowest cost per kilowatt-hour and reject upstream sites inundated by these dams (see Methods). It should be noted that while our method does include several restrictions on total potential (such as costs of population displacement), the actual potential is probably more restricted as other considerations than costs often play a role. For more detail on the methodology, see Methods.

Our assessment distinguishes three different types of hydropower potential: full potential, remaining potential and remaining ecological potential (Table 1). Within each of these categories, a

further distinction was made between technical (<US\$0.50 kWh<sup>-1</sup>) and economic potential (US\$0.10 kWh<sup>-1</sup>). To assess the full potential we systematically explored every river on the globe, assuming that each river was unused and undisturbed. The first 200 km upstream of basin outlets of rivers deeper than 4 m were excluded to allow shipping and other uses (river mouth restriction). Also areas in the vicinity of large bodies of water such as lakes and wide rivers are excluded. We considered this the upper end estimate of the full technical global hydropower potential. The remaining potential is more realistic as it excludes areas already covered by existing dams and reservoirs (listed in the GRanD database<sup>29</sup>) as well as nature protected areas<sup>30</sup>. Additionally, this potential does not allow new hydropower sites downstream of an existing dam if the latter is the first dam (from the river mouth) on a basin main stem. The remaining ecological potential is similar to the remaining potential except that it requires all hydropower stations to release at least 30% of the natural monthly discharge to maintain natural river flow throughout the year<sup>31</sup>. The aim of this 'ecological flow restriction' is to maintain ecological processes (such as fish migration) and allow continued nutrient and sediment transport downstream. Furthermore, dam sites with small reservoirs are given a preference in the final optimization method that can lead to a selection of dam sites that are perhaps more expensive but have less ecological impact.

### Global hydropower potential

Our assessment of the near-global hydropower potential shows a full potential of 13.27 PWh yr<sup>-1</sup> and a remaining potential of 9.49 PWh yr<sup>-1</sup> below US\$0.50 kWh<sup>-1</sup> (Fig. 1a) (US\$0.50 kWh<sup>-1</sup> represents a very high production cost level; current fossil-fuel-based technologies can produce at around US\$0.05–0.1 kWh<sup>-1</sup> without a carbon tax). The difference between these two values (3.78 PWh yr<sup>-1</sup>) approximately covers current global hydropower production (3.7 PWh yr<sup>-1</sup>) (Fig. 2)<sup>9</sup>. This is the global hydropower generation, including the countries north of 60° N latitude. If we exclude Norway (143 GWh yr<sup>-1</sup>), Sweden (78 GWh yr<sup>-1</sup>), Iceland (13 GWh yr<sup>-1</sup>) and Finland (12 GWh yr<sup>-1</sup>), the total current generation is 3.45 PWh yr<sup>-1</sup>. Also Canada and Russia have installed capacity north of 60° N latitude. The remaining ecological potential is estimated at 5.67 PWh yr<sup>-1</sup> below US\$0.50 kWh<sup>-1</sup>, a reduction of 40% compared with the remaining potential without ecological restrictions.

Of the two hydropower systems considered, river power plants make up most of the global remaining potential (65%; see Fig. 1). This is due to their efficient use of the concentrated water flow in the main stems of large catchments, which are found mostly in Asia Pacific, Africa and South America. The reservoir area of all remaining river power sites below a cost of US\$0.10 kWh<sup>-1</sup> is about 240,000 km<sup>2</sup>, in which almost 8 million people currently live. Diversion canal power plants account for 35% of the global remaining potential. These systems are particularly effective in mountainous and populous regions; in Europe, as much as 85% of the regional remaining potential could be captured with this type of system.

Considering that current electricity generation costs by fossil-fired thermal plants and low-cost wind installations are around US\$0.05–0.10 kWh<sup>-1</sup>, the next step is to focus on remaining hydropower potential available at a cost below US\$0.10 kWh<sup>-1</sup> (that is, remaining economic potential, see Table 2). This potential is estimated at 5.70 PWh yr<sup>-1</sup>, to be realized primarily in Asia Pacific (37%), South America (28%) and Africa (25%). Europe (0.20 PWh yr<sup>-1</sup>) and North and Central America (0.36 PWh yr<sup>-1</sup>) together contribute only 10% to this potential; these two regions already use 46% of their full potential (current generation + remaining technical potential). As shown by the steeper cost–supply curves for these regions (Fig. 1d,e), expansion of current hydropower potential in Europe and North America is more difficult than in Africa (current deployment level 5%), South America (23%) or Asia Pacific (30%). The cost curves for these three regions also indicate a greater

**Table 1 | Assessments of the global hydropower potential**

Potential*	Description
Full	Full deployment on all rivers across the globe, excluding only the first 200 km upstream of basin outlets of rivers deeper than 4 m (river mouth restriction) and the area in the vicinity of large bodies of water such as lakes or wide rivers.
Remaining	Similar to full potential, except that: hydropower installations are not allowed in nature protected areas; hydropower production by existing installations is excluded; new hydropower sites are not allowed downstream of the first existing dam on basin main stems.
Remaining ecological restrictions	Similar to remaining potential, except that all hydropower stations are required to release at least 30% of the discharge to maintain natural river flow (ecological flow restriction) and a preference for small reservoirs in the final optimization method that avoids double counting of overlapping reservoirs.

\*Within each category, a further distinction is made between technical potential (<US\$0.50 kWh<sup>-1</sup>) and economic potential (<US\$0.10 kWh<sup>-1</sup>).

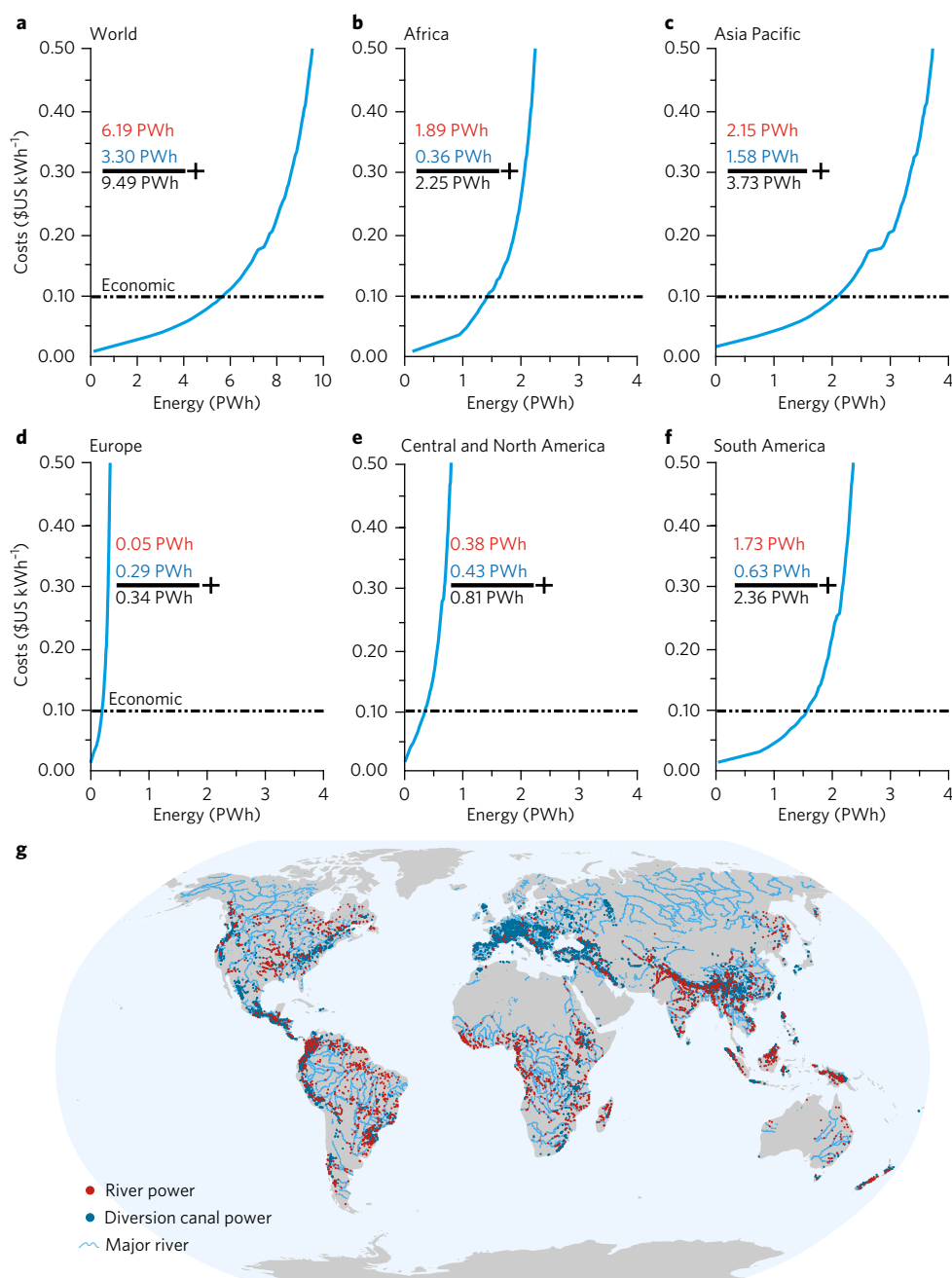


**Fig. 1 | Global and regional cost-supply curves and their geographic locations. a–f**, The global (**a**) and regional (Africa (**b**), Asia Pacific (**c**), Europe (**d**), Central and North America (**e**) and South America (**f**)) cost-supply curves showing the remaining technical potential below US\$0.50 kWh<sup>-1</sup>. The red numbers indicate the total river power potential, the blue numbers the total diversion canal power potential and the black numbers the sum of both. The dot-dashed line indicates the remaining economic potential below a cost of US\$0.10 kWh<sup>-1</sup>. **g**, The geographic locations of the two hydropower systems.

availability of low-cost sites, indicating that future investments in infrastructure and development on hydropower are projected to occur mostly in developing regions. More detail on regional potentials can be found in Supplementary Table 4. Finally, the remaining potential with ecological restrictions below US\$0.10 kWh<sup>-1</sup> is estimated at 3.29 PWh yr<sup>-1</sup>, a reduction of about 42% compared with the remaining economic potential without environmental flow restriction and preference for small reservoirs. Ecological benefits could be further improved by adequate timing of the flow or restricting new sites in main stems. This latter restriction (implemented by excluding new sites in rivers deeper than 4 m) would decrease the ecological economic potential by 34% to 2.17 PWh yr<sup>-1</sup>.

Table 2 compares the results of our assessment to existing estimates in the literature. The latter estimates are all based on runoff-weighted elevation averages at (much) lower resolution (0.5° × 0.5°) than our study and represent a maximum theoretical potential, as they do not account for technical losses in implementation. On the basis of the 0.5° × 0.5° runoff data from the LPjml model, we calculated a global theoretical potential of 50.3 PWh yr<sup>-1</sup>, which is in the middle of the range reported in the literature (30.7–127.6 PWh) (Table 2). However, when using the downscaled data (15° × 15°) and accounting for extraction constraints, we estimate the global potential at 13.27 PWh yr<sup>-1</sup> (full technical potential). This figure lies well below the theoretical estimates reported in the literature.

**Table 2 | Comparison of our global and regional hydropower potential estimates with the literature**

Hydropower potential	Source	Africa	Asia Pacific	Europe <sup>a</sup>	North and Central America	South America	World
Theoretical	Lehner et al. (2005) <sup>11</sup>	-	-	-	-	-	52.25
	Fekete et al. (2010) <sup>10</sup>	-	-	-	-	-	30.67
	Pokhrel et al. (2008) <sup>12</sup>	8.76	23.98	4.17	11.08	10.49	58.48
	Labriet et al. (2013) <sup>13</sup>	9.31	37.24	3.70	15.44	13.05	78.74
	IJHD (2013) <sup>9</sup>	4.43	20.37	2.13	7.60	7.89	42.42
	Zhou et al. (2015) <sup>14</sup>	22.59	54.32	3.76	18.95	27.96	127.58
	Hoes et al. (2017) <sup>15</sup>	7.68	25.11	2.24	7.68	9.73	51.68
	This study	-	-	-	-	-	50.25
Technical	IJHD (2013) <sup>9</sup>	1.58	8.33	0.69	1.89	2.81	15.31
	Zhou et al. (2015) <sup>14</sup>	4.49	12.22	1.37	6.13	6.26	30.47
	Full potential < US\$0.5 kWh <sup>-1</sup>	2.88	4.60	0.61	2.06	3.12	13.27
	Remaining < US\$0.5 kWh <sup>-1</sup>	2.25	3.73	0.34	0.81	2.36	9.49
	Ecological < US\$0.5 kWh <sup>-1</sup>	1.33	2.20	0.24	0.51	1.39	5.67
Economic	IJHD (2013) <sup>9</sup>	0.99	4.83	0.49	1.06	1.68	9.05
	Zhou et al. (2015) <sup>14</sup>	2.92	7.59	0.70	2.90	1.24	15.35
	Full potential < US\$0.1 kWh <sup>-1</sup>	1.99	2.84	0.33	1.41	2.20	8.77
	Remaining < US\$0.1 kWh <sup>-1</sup>	1.44	2.12	0.20	0.36	1.58	5.70
	Ecological < US\$0.1 kWh <sup>-1</sup>	0.77	1.29	0.15	0.23	0.85	3.29
Current generation	IJHD (2013) <sup>9</sup>	0.11	1.63	0.29	0.68	0.71	3.42

Country allocation is fully consistent with the Hydropower Atlas. See Supplementary Table 2 for region definitions.<sup>a</sup>The Hydropower Atlas<sup>9</sup> potentials from Norway, Sweden, Iceland and Finland have been excluded to improve comparability to the results in this paper that consider only regions below 60° N.

Still, our global estimates of full technical potential and remaining economic potential lie in the same range as the bottom-up country-level estimates of technical and economic potential reported by

the Hydropower Atlas<sup>9</sup>. There are some notable differences at the regional level: our estimates for Africa are considerably higher than the estimates provided in the Hydropower Atlas (Table 2). The latter

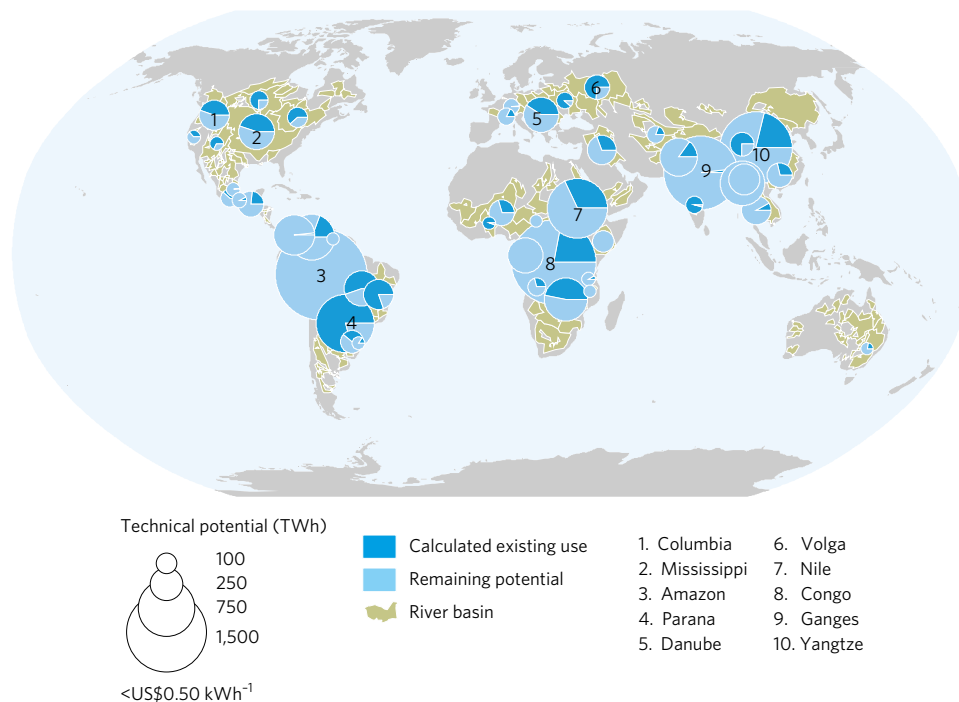


**Fig. 2 | Remaining and calculated existing hydropower potential of the ten largest basins per continent.** Existing use is calculated by placing current hydropower dams as listed in the GRaND database in the river basins as river power systems using their geographical coordinates and dam heights<sup>29</sup>. If the dam height was not available, it was determined using the optimization methodology as described in this paper (see Methods).

are based on national reporting and may suffer from the fact that African countries are relatively 'under-surveyed'. Our estimate of the remaining technical potential in the United States ( $0.27 \text{ PWh yr}^{-1}$  below  $\text{US}\$0.50 \text{ kWh}^{-1}$ , not shown in Table 2) is quite similar to the estimate based on a more detailed study by ORNL<sup>16</sup> ( $0.34 \text{ PWh yr}^{-1}$ ).

### Costs and climate change

In terms of costs, the literature shows a global range of  $\text{US}\$0.02\text{--}0.28 \text{ kWh}^{-1}$  for currently installed hydropower systems, which is consistent with the costs calculated in our study and seems well captured by the cost–supply curves in the economic range in Fig. 1a–f, indicating that the estimates in our assessment are representative<sup>7</sup>.

A sensitivity analysis was applied on the outcome of the economic remaining potential and is shown in Fig. 3a (for details see Supplementary Table 3). The analysis shows that efficiency assumptions most strongly influence the economic remaining potential. The second most influential assumption is the interest rate on capital, clearly showing the capital-intensive character of the hydropower industry. A low interest rate (5%) increases the potential by 26%, while a high interest rate (15%) decreases the potential by 19%. The third most influential parameter is the construction costs. In the cost assessment, we applied the Norwegian and US cost assumptions globally, which could lead to an overestimation of the construction cost in developing regions. Decreasing the construction cost by 50% leads to an 11% increase of the potential.

Human water demand reduces the potential only slightly. Subtracting human water demand from the agriculture, residential, industry and electricity sectors reduces the global remaining technical hydropower potential by 2% ( $0.38 \text{ PWh yr}^{-1}$ ), mostly reducing the potential in Asia Pacific ( $0.30 \text{ PWh yr}^{-1}$ ).

The effect of climate change was analysed using Runoff data for 2050 (30 yr average 2035–2065) from two climate models in the Representative Concentration Pathway (RCP) scenario that leads to  $8.5 \text{ W m}^{-2}$  additional radiative forcing by 2100<sup>32</sup>. This was compared with its historical equivalent (30 yr average 1970–2000) as available in the ISIMIP database<sup>33</sup>. Globally, a slight increase is seen (2–10%) that consistently occurs in Africa (4 to 18%) and Asia Pacific (3 to 6%), while Europe shows a consistent decrease (–2 to –3%).

North and South America are less consistent over across the climate models (Fig. 3b).

### Discussion

Our estimates of global technical and economic hydropower potential are based on site-specific assessment of over 3.8 million sites, using high-resolution discharge and elevation data and cost optimization. The resulting cost–supply curves are a significant step forward from previous studies. Nevertheless, there are reasons why the hydropower potential in the real world may be lower or higher.

To start with the former, our assessment may have overestimated global potential as it does not account for the effects of dams on flow regimes, which may limit downstream hydropower production<sup>34, 35</sup>. Second, our estimates do not account for sediment entrapment within reservoirs, which has been shown to gradually decline storage capacity and hence power production over the years<sup>36</sup>. Third, while our assessment explicitly takes into account the financial costs of population displacement (effectively ruling out reservoirs in densely populated areas), it is likely that social factors will also play other roles that cannot be purely expressed in cost-effectiveness considerations (such as local opposition and vested interests). This will further limit the number of potential dam sites. Fourth, despite the 'river mouth restriction' (Table 1), our calculations may have overestimated the degree to which main river stems can actually be claimed for hydropower production. In our estimate of full technical potential, 24% of all hydropower is supplied by only 500 dam sites (out of more than 60,000 suitable sites). These sites are all located on the main stems of large basins (such as Congo Basin), where large amounts of hydropower can be produced at low cost. However, realization of this potential may be constrained by other uses, such as inland shipping.

Likewise, there are various reasons to assume that our assessment may have underestimated hydropower potential, the remaining potential in particular. First, to evaluate individual dam sites, we calculated optimal dam height based on minimizing production costs, while, in reality, other criteria (such as maximizing power generation) will also play a role in dam design. This may lead to higher dams and hence higher power production. Second,

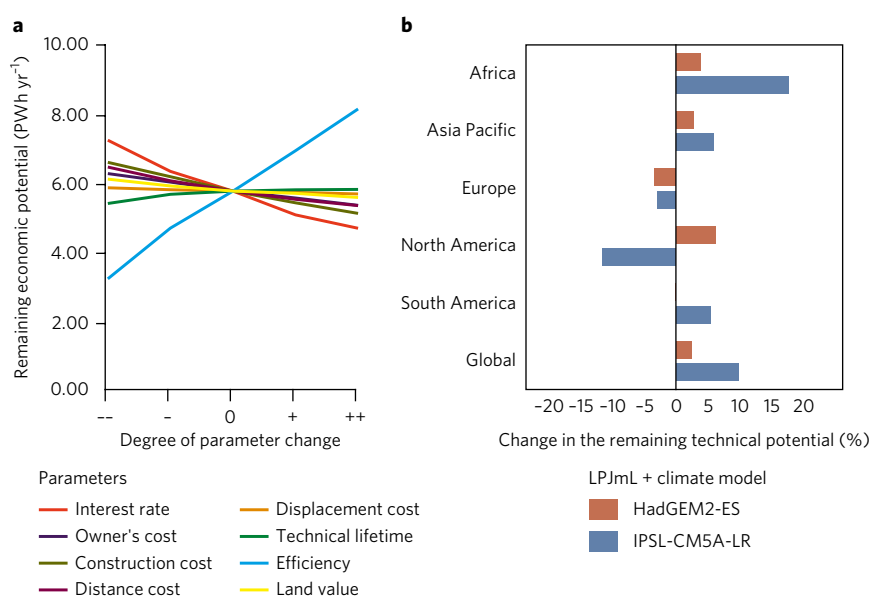


**Fig. 3 | Sensitivity of the remaining potential by parameter settings and climate change.** **a**, Sensitivity runs on the remaining economic potential. See Supplementary Table 3 for definitions of the degrees of parameter change. **b**, The effect of climate change per continent in 2050 (30 yr average 2035–2050) in the RCP 8.5 scenario for different climate models on the remaining technical potential.

if we had selected a smaller distance interval between potential sites (<25 km), we might have identified additional suitable sites with lower production costs. Third, as the HydroSHEDS hydrographic maps and 3"×3" DEM data were not available for high latitudes (>60° N), our estimates do not include potential hydropower production in these northern basins. Fourth, because we globally apply Norwegian and US cost assumptions, we might have overestimated the costs in developing countries. Fifth, our assessment excludes new sites downstream of existing dams on basin main stems, assuming that more dams are not desirable in these river segments. While this assumption may hold for most of the European and North American basins, it may overlook opportunities in African, Asian or South American basins. Sixth, our assessment did not consider river power systems consisting of a set of reservoirs connecting different basins into a single power-producing unit. Such systems allow for economic power production in areas otherwise unsuitable for hydropower production<sup>37</sup>. Finally, our assessment focused on two systems (river power and diversion canal power) that, due to their design, have to spill water during high flows (about three months of the year). If storage power were installed at these sites, annual water flows could be more fully utilized, resulting in higher energy potential. Our assessment did not consider this option because storage power systems have a greater impact on the landscape and flow regime and are generally more expensive as they require larger dams and reservoirs. Reasons to build these systems are dependent on local social and economic conditions, which were outside the scope of our assessment. Examples of reasons to build water storage systems can be for irrigation water storage, shipping navigation improvement, power production flexibility or, when pumped-storage systems are considered, large-scale storage of electricity. These last two forms of hydropower can play a key role in balancing intermittent supply from solar and wind sources. The ecological hydropower potential, as defined in this study, requires more detailed assessment. Real ecological impacts can be evaluated only using site-specific information. Our calculations are only a first estimate of what a set of aggregated rules to minimize ecological impacts would mean. Stricter restrictions on ecological impacts could obviously reduce the overall potential.

The analysis on the effect of climate change is assessed using LPJmL as a global hydrological model (GHM) and two global climate models (GCMs). As has been demonstrated<sup>38</sup>, GCMs clearly are not the only source of uncertainty for hydrological change. The assessment would benefit by including more GHMs and GCMs, as well as more RCP scenarios and a longer time horizon.

Notwithstanding these limitations, our high-resolution assessment provides important information on local to global hydropower potential and associated costs. Rather than providing single figures for technical versus economic potential, our estimates are available in the form of cost–supply curves based on a consistent and transparent methodology. This information can serve as an important input for energy-economy models to further explore the role of hydropower in long-term energy and climate scenarios. Furthermore, our methodology can be used in a broad range of follow-up studies, for example, to assess the impact of hydropower systems on biodiversity and nutrient flows or the impact of climate change on hydropower potential.

## Methods

**Data collection and development.** High-resolution (15"×15") global monthly discharge maps were developed by combining low-resolution (0.5°×0.5°) monthly runoff data (30 yr average 1970–2000) from the hydrological LPJmL model<sup>18–21</sup> with high-resolution (15"×15") area accumulation and drainage direction maps available from the HydroSHEDS project<sup>17</sup>. The downscaling method used here is essentially a discharge routing scheme: the algorithm moves in a generic 'downstream' direction through the landscape, going from areas of lower accumulation to areas of higher accumulation, adding to each grid cell the locally generated runoff and discharge from upstream contributing neighbours.

Water demand from the agriculture, residential, industry and electricity sectors was subtracted in this routing scheme<sup>22,23</sup>. The resulting maps were used to calculate power production and flow duration curves, which in turn were used to determine turbine capacity, reservoir size and load factors.

Individual drainage basins were delineated using the same HydroSHEDS (15"×15") area accumulation and drainage direction maps. However, as opposed to the discharge downscaling method described above, this algorithm moves 'upstream', starting at the highest flow accumulation cell and allocating basin numbers to all upstream neighbouring cells. Next, a hydrological distance map was developed by computing for each grid cell the distance to its basin outlet, measured along the downstream flow paths. The algorithm used here starts at the basin outlets, increasing and assigning distances while moving upstream. This map was used to systematically identify potential hydropower sites at every 25-km river interval in each river basin. This way, we explored >3.8 million potential sites across the globe.

Using HydroSHEDS elevation data, we developed 15"×15" and 3"×3" conditioned digital elevation model (DEM) maps. The 15"×15" DEM maps were used in conjunction with the HydroSHEDS accumulation and drainage direction maps (15"×15") to determine reservoir size and flooded land area, for each potential dam site. The latter was used to calculate the costs of agricultural land loss and population displacement caused by reservoir development (see the Cost estimation section). The 3"×3" DEM maps (which were available from 56° S to 60° N) were used to determine dam height and width (see the Optimization methods section).

A river depth map was derived using an empirical hydraulic geometry equation describing the relation between mean annual discharge and river depth<sup>39</sup>:

$$D_r = 0.23Q^{0.37} \quad (1)$$

where  $D_r$  (m) is river depth and  $Q$  ( $\text{m}^3 \text{s}^{-1}$ ) is the mean annual discharge. This relationship was obtained in the Columbia River Basin in the US with 264 empirical measurements on discharge, river depth and river width ( $R^2=0.67$ ). The resulting map was used to correct the head and tail water elevation of each dam.

To obtain a 15"×15" population density map, we resized the 30"×30" LandScan global population map<sup>40</sup> by multiplying the original raster with a factor 2 and dividing each cell by 2<sup>2</sup>. This map was used to assess the number of people that would be displaced as a result of hydropower reservoirs.

To calculate the cost of agriculture land loss caused by reservoir construction, we developed a land value map (15"×15") based on the potential agricultural yield map from the IMAGE 3.0 model<sup>27</sup>. The latter map (0.5°×0.5°) indicates potential annual rain-fed production (tons  $\text{km}^{-2}$ ) of the seven most produced crops worldwide in 2010: temperate cereals, rice, maize, tropical cereals, roots and tubers, pulses and oil crops. Following the method by Kunte, Hamilton<sup>41</sup>, we estimated land value (US\$  $\text{km}^{-2}$ ) for each cell by converting the sum of the annual production over an infinite period to the present value using the default discount factor in this study (10%). If multiple crops were grown within the same cell, the crop with the highest average price was selected. In the case of temperate cereals, rice and maize, average global commodity prices were derived from the World Bank database<sup>42</sup>. For the remaining crop groups, we used the 10-year average national commodity price of FAOSTAT<sup>43</sup>. For countries that lack data, a weighted-average approach was used, selecting the price in the main producing country combined with a weighted-average approach to account for the different crops within each crop group (see Supplementary Table 4).

A distance-to-power line map was developed using power line data from the OpenStreetMap project, which provides shape files with a global coverage<sup>44</sup>. To our knowledge, this is the only publicly available data set on global power lines. We converted these shape files to a global 30"×30" raster and applied them to an algorithm to calculate the distance (km) between a potential hydropower site and its nearest power line. Next, we used this distance, in combination with the calculated local turbine capacity, as input in a power line allocation scheme<sup>25</sup> to select the required cable type and calculate the investment costs of building new transmission lines (see the Cost estimation section).

A seismic hazard map was applied using data from the global seismic hazard map produced by the Global Seismic Hazard Program<sup>45</sup>. Seismic hazard is expressed as a 10% probability that a certain peak ground acceleration value ( $\text{m s}^{-1}$ ) is exceeded in 50 years. These data were used to assess the seismic risk of individual dam sites.

Finally, we applied a map of protected areas using data from the World Database of Protected Areas (WDPA)<sup>30</sup>. This database classifies areas in different protection categories based on land management objectives. In our assessment of remaining hydropower potential (see Table 1 in the main text), we explicitly excluded protected areas as defined in WDPA categories I and II (Strict Nature Reserve, Ia; Wilderness Area, Ib; and National Park, II), including a 10 km buffer zone.

**Cost estimation.** To assess global technical and economic hydropower potential, we considered two hydropower systems: river power plants and diversion canal power plants (following the definitions in Wagner and Mathur<sup>24</sup>). To assess the (system- and site-specific) costs of each of these systems, we used planning tools developed by the Norwegian and US hydropower industry<sup>25,26</sup>. The industry uses these tools to calculate foreseeable contractor and supplier costs in early

stages of a project, based on cost equations derived from hydropower tenders and contracts. We used the spatial information described in the Data Collection and Development section as input for these cost equations (Supplementary Table 5), allowing site-specific cost estimation based on a variety of physical parameters such as discharge and elevation.

As Supplementary Table 5 shows, most cost components are directly related to hydropower plant construction. Investments are annualized using a discount factor of 10% and economic lifetime of 40 years<sup>7</sup>. The turbine cost equation taken from IRENA<sup>7</sup> is a direct function of turbine capacity and enables us to estimate turbine cost without having to specify the type of turbine. Turbine capacity, which itself is a direct function of the discharge in the grid cell, also plays a role in various other cost components. For example, power line costs indirectly depend on turbine capacity, because the latter determines the type of cable required. We used the allocation scheme of Veileder<sup>25</sup> to select cable type and calculate the resulting power line construction costs per kilometre, accounting for transmission distance using the distance-to-power line map<sup>14</sup>. Dam construction costs for river power systems are directly related to dam height ( $D_H$ ) and dam width ( $D_W$ ), which we estimated using high-resolution 3"×3" DEM data. The piping costs for diversion canal power systems consist of two components (head race tunnel and penstock), which both depend on pipe surface area ( $A_P$ ) and pipe length ( $L_P$ ). We calculated required pipe length using the 15"×15" DEM maps, and optimized pipe diameter based on trade-offs between construction costs and friction losses (see the Optimization methods section).

The costs of agricultural land loss and population displacement are the only cost components directly related to the area of land inundated by a hydropower reservoir (Supplementary Table 5). The first was estimated using the land value map, which we developed on the basis of the IMAGE 3.0 land use model and FAOSTAT and World Bank commodity prices (see the Data collection and development section). The second was estimated using the population density map (derived from LandScan maps, see the Data collection and development section), multiplying the number of displaced people by two times the GDP (Gross domestic product; current) per capita of the country in question (using GDP data from WorldBank<sup>46</sup>). This multiplication factor of 2 is derived from two publications on various hydropower projects in China and Paraguay<sup>47,48</sup>. We realize that this value is uncertain and might be too low for developed countries, but literature on displacement costs is scarce.

**Hydropower production.** To calculate the energy production at each (potential) hydropower site, we used different equations for the two systems considered. For river power plants, energy production (Wh) was calculated as follows:

$$E_{RP} = \rho g (Z_1 - Z_2) Q_D \times (t) \times LF_{RP} \eta_{ww} \quad (2)$$

where  $\rho$  is water density ( $\text{kg m}^{-3}$ ),  $g$  is gravitational acceleration ( $9.8 \text{ m s}^{-2}$ ),  $Z_1$  is head water elevation (m),  $Z_2$  is tail water elevation (m),  $Q_D$  is the design discharge ( $\text{m}^3 \text{ s}^{-1}$ ),  $t$  is the number of operational hours per year,  $LF_{RP}$  is the yearly load factor, and  $\eta_{ww}$  is the water-to-wire efficiency (70%). The difference between head water elevation ( $Z_1$ ) and tail water elevation ( $Z_2$ ) determines the head of the dam. Head water elevation is equal to dam height, while tail water elevation is a function of river depth. We calculated the latter based on an empirical relation between river depth and discharge (see the Data collection and development section and equation (1)). The design discharge ( $Q_D$ ), which is used to determine turbine size, is defined as the fourth highest discharge month in the flow duration curve of the grid cell, allowing for 30% exceedance<sup>16</sup>. Turbine size determines the load factor ( $LF_{RP}$ ) and is location specific.

For diversion canal power plants, energy production (Wh) was calculated as follows:

$$E_{DP} = \rho g (Z_{in} - Z_{ps} - h_f) Q_D \times (t) \times LF_{DP} \eta_t \quad (3)$$

where  $\rho$  is water density ( $\text{kg m}^{-3}$ ),  $g$  is gravitational acceleration ( $9.8 \text{ m s}^{-2}$ ),  $Z_{in}$  is the elevation of the water inlet,  $Z_{ps}$  is the elevation of the power station,  $h_f$  is the head loss,  $Q_D$  is the design discharge at the inlet location ( $\text{m}^3 \text{ s}^{-1}$ ),  $t$  is the number of operational hours per year,  $LF_{DP}$  is the load factor (related to  $Q_D$ ) and  $\eta_t$  is the turbine efficiency (90%). Similarly to river power plants, the design discharge ( $Q_D$ ) of diversion canal power plants determines turbine size and is calculated using the flow duration curve of the grid cell, allowing for 30% exceedance. The gross head of the system is determined by elevation difference minus the head loss friction factor. This loss factor ( $h_f$ ), which accounts for friction losses in the pipes connecting the inlet to the power station, was calculated in an iterative approach using the Darcy–Weisbach (equation (4)) and Colebrook–White (equation (5)) equations:

$$h_f = f_D \frac{L}{D} \frac{v^2}{2g} \quad (4)$$

where  $h_f$  is the head loss (m),  $f_D$  is the Darcy friction factor,  $L$  is pipe length (m),  $D$  is pipe hydraulic diameter (m), and  $v$  is the flow velocity ( $\text{m s}^{-1}$ ). The Darcy friction factor ( $f_D$ ) was calculated using the Colebrook–White equation:

$$\frac{1}{\sqrt{f_D}} = -2 \log_{10} \left( \frac{\epsilon}{3.7D} + \frac{2.51}{\text{Re} \sqrt{f_D}} \right) \quad (5)$$

where  $\epsilon$  is the roughness height (m) and  $\text{Re}$  is the Reynolds number. Pipe length ( $L$ ) depends on the distance between the inlet location and the power station, derived from the 15"×15" DEM maps. Pipe hydraulic diameter ( $D$ ) and flow velocity ( $v$ ) depend on the available discharge and financial trade-offs (see the Optimization section). Roughness height ( $\epsilon$ ) was set at 2 mm to represent a piping system consisting of a tailrace tunnel made of rough concrete and a penstock made of steel. The penstock length is the same as the gross head.

**Optimization methods.** To design the dimensions of the hydropower systems at each site, we used three optimization processes: to determine the optimal dam height of river power plants, to determine the optimal number and diameter of the pipes of diversion canal power plants, and to determine the best inlet location for these pipes. A fourth optimization process was used to select the best (cost-optimal) dam sites to avoid double counting of overlapping reservoirs.

To start with dam height of river power systems, this is the most important variable because it determines not only the head and therefore the energy production, but also the construction and reservoir costs (including costs of population displacement and agricultural land loss caused by reservoir construction). The optimal trade-off between energy production and costs was determined by stepwise increasing dam height, taking into account local topography while keeping track of the total costs. This optimization process is illustrated in Supplementary Fig. 1. The algorithm starts with identifying a potential dam site using the hydrological distance map and monthly discharge data (see the Data collection and development section). On this site, a dam is evaluated (indicated by the red dot in Supplementary Fig. 1) using the high-resolution (3"×3") DEM map. In this process, dam height is increased stepwise while keeping track of the dam width required to seal off the river valley up to the dam height considered. This dam height determines the reservoir size, which is calculated using the flow accumulation and flow direction maps. Reservoir size, in turn, determines the inundated land area and hence the costs of population displacement and agricultural land loss. Finally, power line cost (a function of the distance to the nearest power line and the required cable type) is added as a fixed cost component to the cost model. The sum of all cost components divided by the energy production as a function of dam height is shown in the top graph of Supplementary Fig. 1. When dam height (and hence, head) is low, energy production is also low, resulting in a relatively high generation price ( $\text{US\$ kWh}^{-1}$ ) due to the fixed cost components. As dam height (head) increases, the generation price is driven down by the increasing power production. At some point, however, the total costs increase faster than the power production such that an optimum point is reached. In this particular example, population displacement costs play a key role in determining the optimum dam height.

The second optimization process was applied to determine the optimal (site-specific) dimensions of the piping system of diversion canal power plants. These pipes connect a water inlet at higher elevation to a power station at lower elevation; they can be up to several kilometres long and form an important part of the total costs. Piping costs are a direct function of pipe length and diameter (see the cost equations in Supplementary Table 1), but are also influenced by friction losses (equations (4) and (5)): a narrow pipe may be cheaper to build but also causes more friction, leading to head loss and hence lower energy production. To account for these financial trade-offs, we used an optimization algorithm based on acceptable head loss to select the least-cost option among three different pipe diameters (1, 2 and 3 m)<sup>16</sup>.

The third optimization process focused on identifying the best inlet locations for the pipes of diversion canal power plants. This process is illustrated in Supplementary Fig. 2 for a site (indicated by the red dot) in the Indus Basin, Pakistan. The algorithm starts with selecting a range of potential inlet sites (indicated by small blue and white dots) along natural streams (discharge  $> 0.2 \text{ m}^3 \text{ s}^{-1}$ ) at six different elevation levels in the upstream area of the power station. For each of these inlet sites, a complete cost assessment is made; the most economic site is selected (indicated by the larger blue and white dots). The upstream and downstream discharge of this site is reserved, after which the selection process is repeated to check for additional cost-effective inlet sites.

Finally, the fourth optimization process was applied to avoid double counting of overlapping reservoirs. Overlapping reservoirs occurred as a 'side-effect' of our approach to assign potential dam sites at every 25-km river interval. While this approach allowed a systematic exploration of hydropower potential in each basin, some of the assigned dams resulted in reservoirs extending far beyond 25 km, inundating upstream dams. To select the best dam sites in these cases, we explored four criteria: costs, potential, proportional cost-potential (1:1) and cost per kilowatt-hour. The cost per kilowatt-hour approach gave the best results (the lowest curve in the cost-effective range of the supply curve) and was used in this assessment. Thus, dam sites with the lowest cost per kilowatt-hour were given priority; any upstream sites inundated by these dams were removed from the supply curve.

The interplay of the four optimization processes is graphically depicted in Supplementary Fig. 3, showing existing reservoirs (green dots) deselecting potential dam sites (light blue dots) and a collection of suitable locations (river power and diversion canal power) that together represent the remaining hydropower potential. The pink dot is a dam site that has been deselected by a downstream reservoir.

**Data availability.** The data that support the plots within this paper and other findings of this study are available from the corresponding author upon reasonable request.

Received: 1 December 2016; Accepted: 10 August 2017;

Published online: 18 September 2017

## References

- World Energy Outlook (International Energy Agency, Paris, 2016).
- Hoogwijk, M. M. *On The Global And Regional Potential Of Renewable Energy Sources*. PhD thesis, Universiteit Utrecht, Faculteit Scheikunde (2004).
- Köberle, A. C., Gernaat, D. E. H. J. & van Vuuren, D. P. Assessing current and future techno-economic potential of concentrated solar power and photovoltaic electricity generation. *Energy* **89**, 739–56 (2015).
- Pietzcker, R. C., Stetter, D., Manger, S. & Luderer, G. Using the Sun to decarbonize the power sector: The economic potential of photovoltaics and concentrating solar power. *Appl. Energy* **135**, 704–20 (2014).
- Arent, D. et al. *Improved Offshore Wind Resource Assessment in Global Climate Stabilization Scenarios* Contract No. NREL/TP-6A20-55049 (NREL; 2012).
- World Energy Resources: Hydropower* (World Energy Council, 2013).
- Renewable Energy Technologies: Cost Analysis Series* (IRENA, 2012).
- IPCC *Special Report on Renewable Energy Sources and Climate Change Mitigation: Hydropower* (IPCC, 2011).
- The International Journal on Hydropower & Dams. *World Atlas & Industry Guide* (Wallington, UK, 2013).
- Fekete, B. M. et al. Millennium ecosystem assessment scenario drivers (1970–2050): Climate and hydrological alterations. *Glob. Biogeochem. Cycles* **24**, GB0A12 (2010).
- Lehner, B., Czisch, G. & Vassolo, S. The impact of global change on the hydropower potential of Europe: A model-based analysis. *Energy Policy* **33**(7), 839–55 (2005).
- Pokhrel, Y. N., Oki, T., Kanae, S. A grid based assessment of global theoretical hydropower potential. *Ann. J. Hydraul. Eng.* **52**, 712 (2008).
- Labriet, M. et al. *Uncertainty analyses in TIAM, ERMITAGE WP8 Climate and Energy/Technology Deliverable 8.1* (2013).
- Zhou, Y., Hejazi, M., Smith, S., Edmonds, J., Li, H. & Clarke, L. et al. A comprehensive view of global potential for hydro-generated electricity. *Energy Environ. Sci.* **8**, 2622–2633 (2015).
- Hoes, O. A., Meijer, L. J., Van Der Ent, R. J. & Van De Giesen, N. C. Systematic high-resolution assessment of global hydropower potential. *PLOS ONE*. **12**, e0171844 (2017).
- New Stream-reach Development: A Comprehensive Assessment of Hydropower Energy Potential in the United States* (Oak Ridge National Laboratory, Oak Ridge, 2014).
- Lehner, B., Verdin, K. & Jarvis, A. New global hydrography derived from spaceborne elevation data. *Eos, Trans. AGU* **89**, 93–94 (2008).
- Bondeau, A. et al. Modelling the role of agriculture for the 20th century global terrestrial carbon balance. *Glob. Change Biol.* **13**, 679–706 (2007).
- Biemans, H. et al. Effects of precipitation uncertainty on discharge calculations for main river basins. *J. Hydrometeorol.* **10**, 1011–25 (2009).
- Rost, S. et al. Agricultural green and blue water consumption and its influence on the global water system. *Water Resour. Res.* <http://dx.doi.org/10.1029/2007WR006331> (2008).
- Gerten, D., Schaphoff, S., Haberlandt, U., Lucht, W. & Sitch, S. Terrestrial vegetation and water balance—hydrological evaluation of a dynamic global vegetation model. *J. Hydrol.* **286**, 249–70 (2004).
- Biemans, H. et al. Future water resources for food production in five South Asian river basins and potential for adaptation—A modeling study. *Sci. Total Environ.* **468**, S117–S31 (2013).
- Bijl, D. L., Bogaart, P. W., Kram, T., de Vries, B. J. & van Vuuren, D. P. Long-term water demand for electricity, industry and households. *Environ. Sci. Policy* **55**, 75–86 (2016).
- Wagner, H.-J., Mathur, J. *Introduction to Hydro Energy Systems — Basics, Technology and Operation* (Springer, Berlin Heidelberg, 2011).
- Cost Base for Hydropower Plants (with a Generating Capacity of More than 10 000 kW)* (Norwegian Water Resources and Energy Directorate (NVE), Oslo, 2012).
- Hall, D. G., Hunt, R. T., Reeves, K. S., Carroll, G. R. *Estimation of Economic Parameters of US Hydropower Resources* Contract No. INEEL/EXT-03-00662 (Idaho National Engineering and Environmental Laboratory, 2003).
- Stehfest, E. et al. *Integrated Assessment of Global Environmental Change with IMAGE 3.0 - Model Description and Policy Applications* (PBL The Netherlands Environmental Assessment Agency, 2014).
- FAOSTAT *Database Collections* (Food and Agriculture Organization of the United Nations, 2013).
- Lehner, B. et al. High resolution mapping of the world's reservoirs and dams for sustainable river flow management: GRAND Database (V1.0). *Front. Ecol. Environ.* **9**, 494–502 (2011).
- The World Database on Protected Areas (WDPA)* (UNEP-WCMC, Cambridge, UK, 2015).
- Janse, J. et al. GLOBIO-Aquatic, a global model of human impact on the biodiversity of inland aquatic ecosystems. *Environ. Sci. Policy* **48**, 99–114 (2015).
- Riahi, K. et al. RCP 8.5—A scenario of comparatively high greenhouse gas emissions. *Climatic Change* **109**, 33 (2011).
- Warszawski, L. et al. The inter-sectoral impact model intercomparison project (ISI-MIP): project framework. *Proc. Natl Acad. Sci. USA* **111**, 3228–32 (2014).
- Ziv, G., Baran, E., Nam, S., Rodríguez-Iturbe, I. & Levin, S. A. Trading-off fish biodiversity, food security, and hydropower in the Mekong River Basin. *Proc. Natl Acad. Sci. USA* **109**, 5609–5614 (2012).
- Magilligan, F. J. & Nislow, K. H. Changes in hydrologic regime by dams. *Geomorphology* **71**, 61–78 (2005).
- Wisser, D., Frohling, S., Hagen, S. & Bierkens, M. F. Beyond peak reservoir storage? A global estimate of declining water storage capacity in large reservoirs. *Water Resour. Res.* **49**, 5732–5739 (2013).
- House, N., House, H., House, D., Hafen, T., House, R. *Power from the Glens* (Scottish Hydro Electric, 2005).
- Hagemann, S. et al. Climate change impact on available water resources obtained using multiple global climate and hydrology models. *Earth Syst. Dynam.* **4**, 129–44 (2013).
- Magirl, C. S., Olsen, T. D. *Navigability Potential of Washington Rivers and Streams Determined with Hydraulic Geometry and a Geographic Information System* Contract No. 5122 (U.S. Department of the Interior & US Geological Survey, 2009).
- Bright, E. A., Coleman, P. R. & Rose, A. N. *Landscan 2010* (Oak Ridge National Laboratory, Oak Ridge, TN, 2011).
- Kunte, A., Hamilton, K., Dixon, J. & Clemens, M. *Estimating National Wealth: Methodology and Results* (Environment Department, 1998).
- Commodity Price Data (The Pink Sheet)* (World Bank, 2015).
- Annual Producer Prices* (Food and Agriculture Organization of the United Nations, 2015).
- Project Power Networks* (OpenStreetMap, 2015).
- Harris, J., Bonneville, D., Kersting, R. A., Lawson, J. & Morris, P. *Cost Analyses and Benefit Studies for Earthquake-Resistant Construction in Memphis, Tennessee* Report 14-917-26 (NISTGCR, 2013).
- Global Economic Monitor* (World Bank, 2014).
- Jackson, S. & Sleight, A. Resettlement for China's Three Gorges Dam: socio-economic impact and institutional tensions. *Communist Post-Communist Stud.* **33**, 223–41 (2000).
- Cernea, M. M. *The Economics of Involuntary Resettlement — Questions and Challenges* (World Bank, 1999).

## Acknowledgements

C. Ettema is acknowledged for editing part of the manuscript. Moreover, the study benefited from FP7/2007-2013 financial support under grant agreement number 308329 (ADVANCE).

## Author Contributions

D.E.H.J.G. and P.W.B. conceived the idea and developed the modelling techniques. D.P.v.V. assisted in refining the idea and manuscript. H.B. provided climate input data and R.N. assisted in preparatory analyses. D.E.H.J.G. drafted the manuscript. All authors discussed the results and contributed to the manuscript.

## Additional information

**Supplementary information** is available for this paper at doi:10.1038/s41560-017-0006-y.

**Reprints and permissions information** is available at [www.nature.com/reprints](http://www.nature.com/reprints).

**Correspondence and requests for materials** should be addressed to D.E.H.J.G.

**Publisher's note:** Springer Nature remains neutral with regard to jurisdictional claims in published maps and institutional affiliations.